REPORT No. 296

PRESSURE DISTRIBUTION TESTS ON PW-9 WING MODELS FROM −18° THROUGH 90° ANGLE OF ATTACK

By OSCAR E. LOESER, Jr.

Langley Memorial Aeronautical Laboratory

REPORT No. 296

PRESSURE DISTRIBUTION TESTS ON PW-9 WING MODELS FROM −18° THROUGH 90° ANGLE OF ATTACK

By Oscar E. Loeser, Jr.

SUMMARY

At the request of the Army Air Corps, an investigation of the pressure distribution over P W-9 wing models was conducted in the atmospheric wind tunnel of the National Advisory Committee for Aeronautics. The primary purpose of these tests was to obtain wind-tunnel data on the load distribution on this cellule to be correlated with similar information obtained in flight tests, both to be used for design purposes. Because of the importance of the conditions beyond the stall as affecting control and stability, this investigation was extended through 90° angle of attack. The results for the range of normal flight have been given in N. A. C. A. Technical Report No. 271. The present paper presents the same results in a different form and includes, in addition, those over the greater range of angle of attack, −18° through 90°.

The results show that—

At angles of attack above maximum lift, the biplane upper wing pressures are decreased by the shielding action of the lower wing.

The burble of the biplane lower wing, with respect to the angle of attack, is delayed, due to the influence of the upper wing.

The center of pressure of the biplane upper wing (semispan) is, in general, displaced forward and outward with reference to that of the wing as a monoplane, while for the lower wing there is but slight difference for both conditions.

The overhanging portion of the upper wing is little affected by the presence of the lower wing.

INTRODUCTION

The increased speeds and maneuverability of modern pursuit airplanes call for careful consideration of design and of wing loads over a large range of angle of attack. Similarly, the consideration being given to stability and control above the stall requires an extension of the usual range of pressure distribution investigations. To this end, at the request of the Army Air Corps, the distribution of pressure over the wing models of a modern pursuit airplane, PW-9, has been investigated in the atmospheric wind tunnel of the National Advisory Committee for Aeronautics (Reference 1). The test results were given in part in N. A. C. A. Technical Report No. 271 (Reference 2). In the present paper the pressures are plotted (normal to the chord) as resultant or total pressures from −18° through 90° angle of attack, while in the former report they were plotted as individual upper and lower surface pressures in the conventional manner over the range of normal flight.

APPARATUS AND METHODS

Half-span, laminated wooden models accurate to ±0.003-inch, with inlaid pressure tubes of 0.032-inch bore, were used in this investigation. (Fig. 1.) These models were 1:9.6 scale of the PW-9 airplane cellule and of Göttingen 436 airfoil section throughout. (Fig. 2.) The most unusual features of this biplane cellule are the difference in plan form of the wings and the increased angle of incidence of the center section. Three-foot to four-foot lengths of $\frac{3}{16}$-inch, inside diameter, rubber tubing served to connect the pressure tubes of the manometer.

Compensation was made for the missing half span by means of a reflecting plane. (Figs. 3 and 4.) Static and dynamic pressure surveys were made normal to this plane two chord lengths ahead of the models, and, as expected, the velocity close to the plane was found lower than that in the free stream above it. This condition was remedied by slightly bending the leading edge of the reflecting plane downward.

The integrated mean pressures of the final surveys were used to calibrate a Pitot static tube, located 3 feet ahead of the honeycomb, forward of the test section. This tube was then used to maintain an air speed of approximately 30 meters per second.

Göttingen 436 airfoil

Station per cent chord	Upper per cent chord	Lower per cent chord
0	2.85	2.85
1¼	4.59	1.21
2½	5.54	0.69
5	6.86	0.37
7½	8.02	0.21
10	8.92	0.05
15	10.03	0.00
20	10.82	0.00
30	11.08	0.00
40	10.55	0.00
50	9.60	0.00
60	8.28	0.00
70	6.60	0.00
80	4.70	0.00
90	2.59	0.00
95	1.43	0.00
100	0.26	0.00
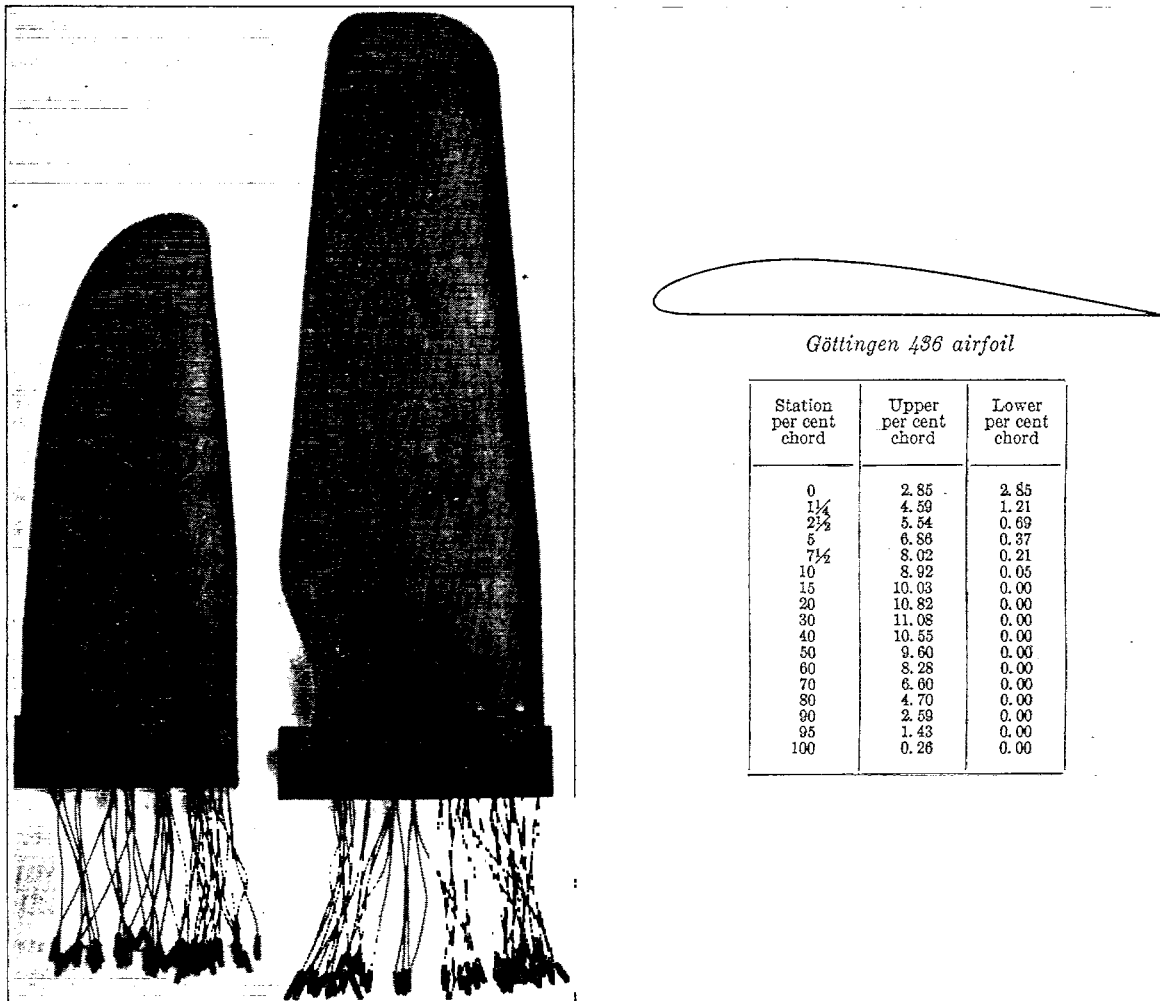
FIG. 1.—PW-9 Pressure-distribution wing models

In calculating the results, no allowance was made for the change in dynamic and static pressure with increasing angle of attack due to the blocking of the air stream by the models, since an evaluation of this effect would have required a separate investigation. Consequently, above maximum lift the accuracy of the results may be expected to decrease slightly.

To obtain a pressure distribution record as shown in Figure 5, the model was set at the desired angle of attack and an exposure made upon a sheet of photostat paper held against the manometer tubes, after a constant condition of pressures had been obtained. The recorded pressures were then scaled off accurately, tabulated, and plotted to obtain the individual test section pressure distribution curves. A comprehensive discussion of airfoil pressure distribution principles is given in Reference 3.
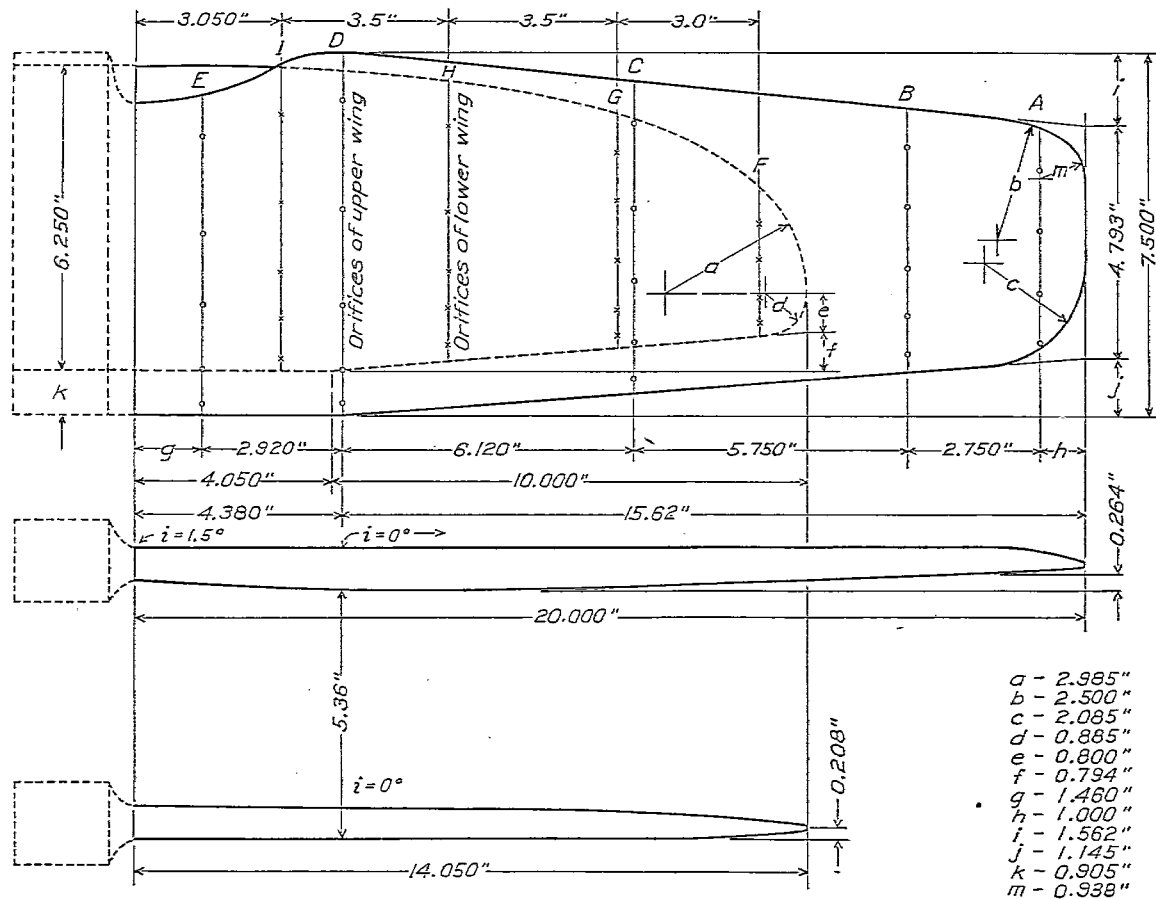
FIG. 2.—Plan and front elevation of PW-9 wing models.   Göttingen 436 airfoil
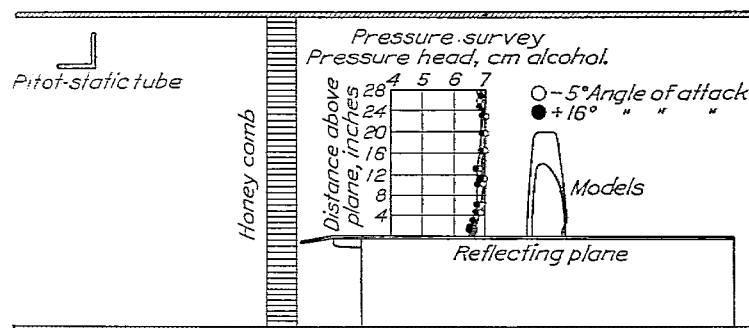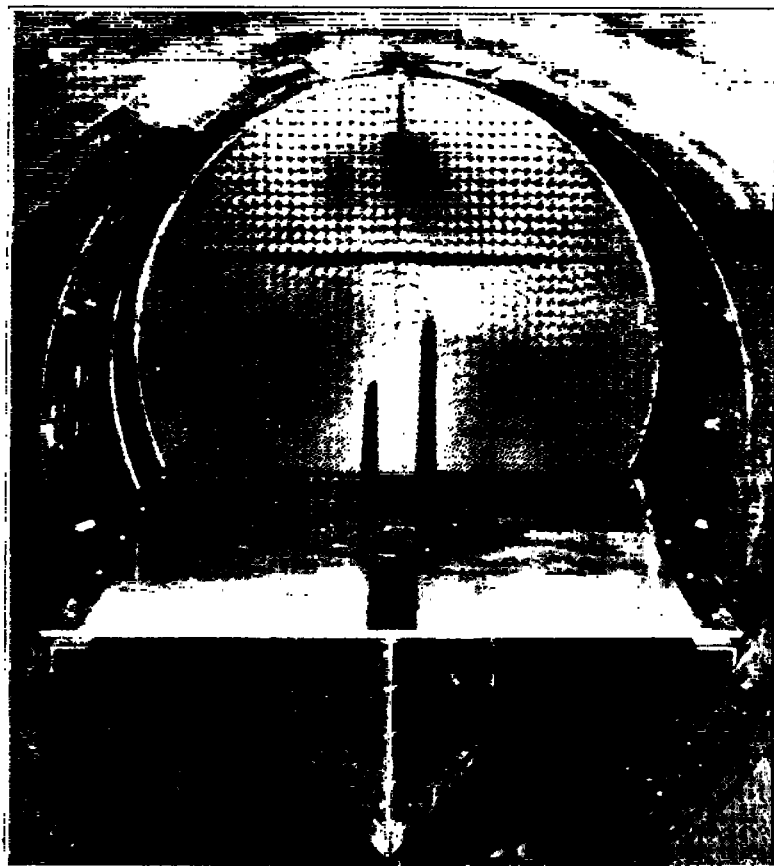

FIG. 3.—Longitudinal section of wind tunnel

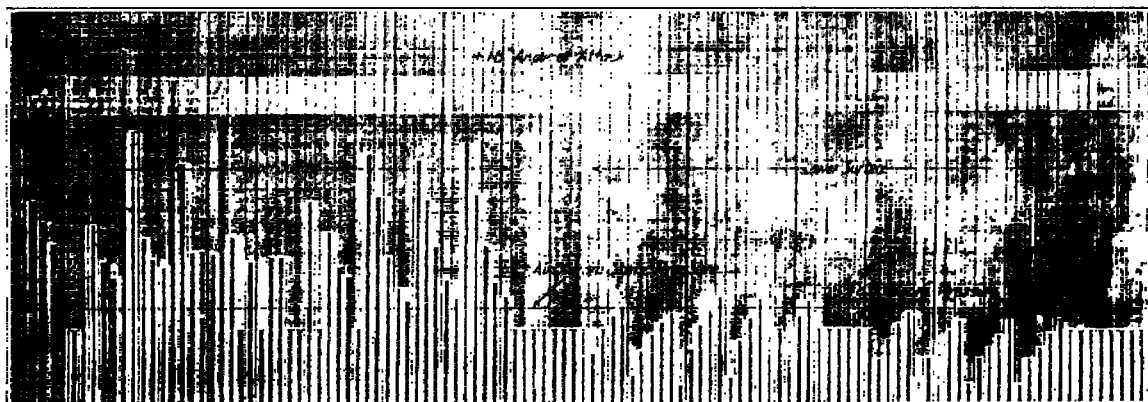FIG. 4.—PW-9 wing models in wind tunnel

FIG. 5.—Reduced photograph of a manometer record

The final curves are estimated to be accurate to within about ±3 per cent, for the planimetering of the pressure distribution curves was held to within 1 per cent, while the fairing of the curves was susceptible to errors of possibly 2 to 3 per cent.

The Reynolds Number based on the weighted mean chord was approximately 300,000.

RESULTS

It was possible to obtain the resultant normal pressures directly from the algebraic difference of the recorded surface pressures, inasmuch as the upper surface orifices were located directly above the corresponding orifices in the lower surface of each wing. These resultant pressures in terms of dynamic pressure,

$$q = \frac{1}{2}\rho V^2$$

where
ρ = air density

V = air speed

for the wing models separately and in their mutual relation in the biplane cellule, were plotted as ordinates in their respective positions on the isometric projection of the wings. (Figs. 6–18.) The pressure diagrams are drawn through the test points in every case; but in order to avoid congestion these points are not shown. This manner of presentation of pressure distribution offers a direct comparison of pressures between the various test sections over the wing, and also between the monoplane and biplane pressures.

Variation of the coefficient of normal force C_{NF_1}, at each test section along the semispan, is shown in Figures 19 and 20. C_{NF_1} is the mean pressure in terms of q of the individual test sections.

Figure 21 illustrates the variation of coefficient of normal force, C_{NF}, for each wing and for the biplane cellule; with change of angle of attack. The value of C_{NF} was obtained from the integrated mean of the respective C_{NF_1} curves. That for the biplane cellule was obtained from the weighted sum of C_{NF} for both wings.

$$C_{NF_b} = C_{NF_u} \times \frac{S_u}{S_t} + C_{NF_l} \times \frac{Sl}{S_t}$$

C_{NF_b} = normal force coefficient for the biplane cellule.
C_{NF_u} = normal force coefficient for the biplane upper wing.
C_{NF_L} = normal force coefficient for the biplane lower wing.
S_u = area of upper wing.
S_L = area of lower wing.
S_T = total area of both wings.

The distribution of load along the span, in terms of a nondimensiona coefficient K, is shown in Figures 22 and 23.

$$K = \frac{C_{NF} \times \text{chord}}{\text{mean chord}}$$

Due to the irregular plan form of the wings, the longitudinal center of pressure C_p, positions were plotted on the mean chord of each wing in their respective positions in the biplane. (Fig. 24.) The mean chord was obtained by dividing the area by the span, and the mean C_p was derived from the integrated mean of the C_p curves as plotted on the isometric diagrams. The biplane cellule center of pressure was computed as the equivalent moment arm of the forces on both wings from the center section leading edge of the upper wing:

$$C_{p_b} = \frac{C_{NF_u} \times S_u \times a + C_{NF_l} \times S_l \times b}{C_{NF_u} \times S_u + C_{NF_u} \times S_l}$$

C_{p_b} = center of pressure of biplane cellule.
a = position of C_p of upper wing back of center section leading edge.
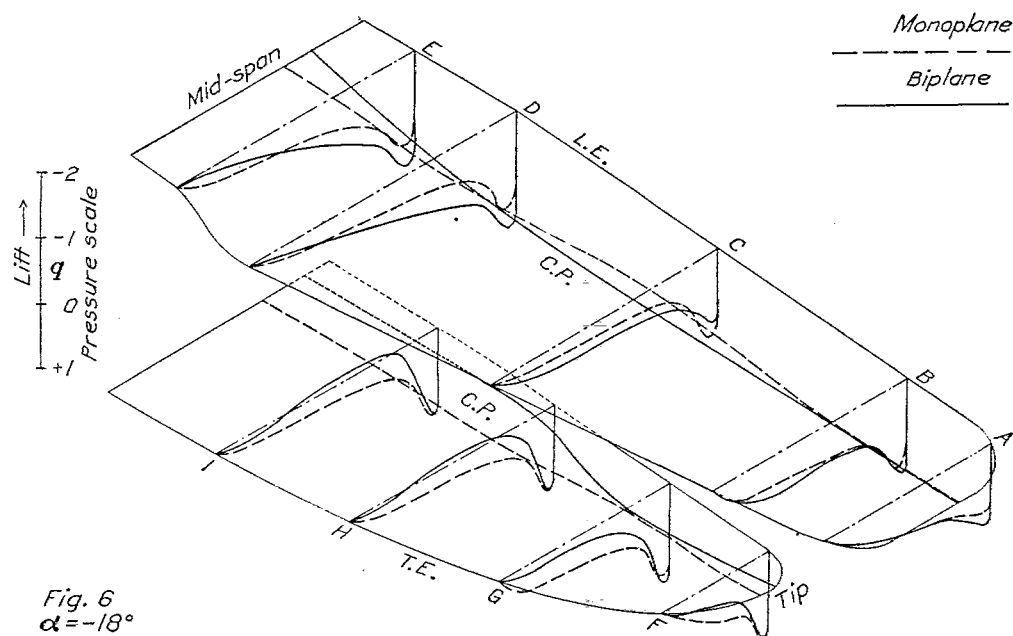b = position of C_p of lower wing back of upper wing center section leading edge.
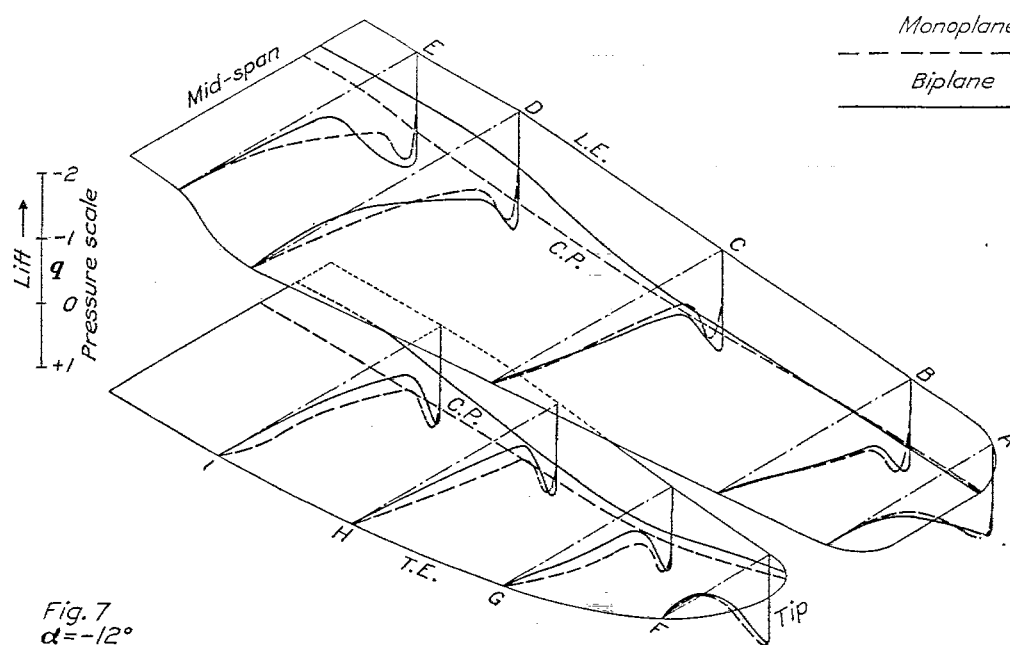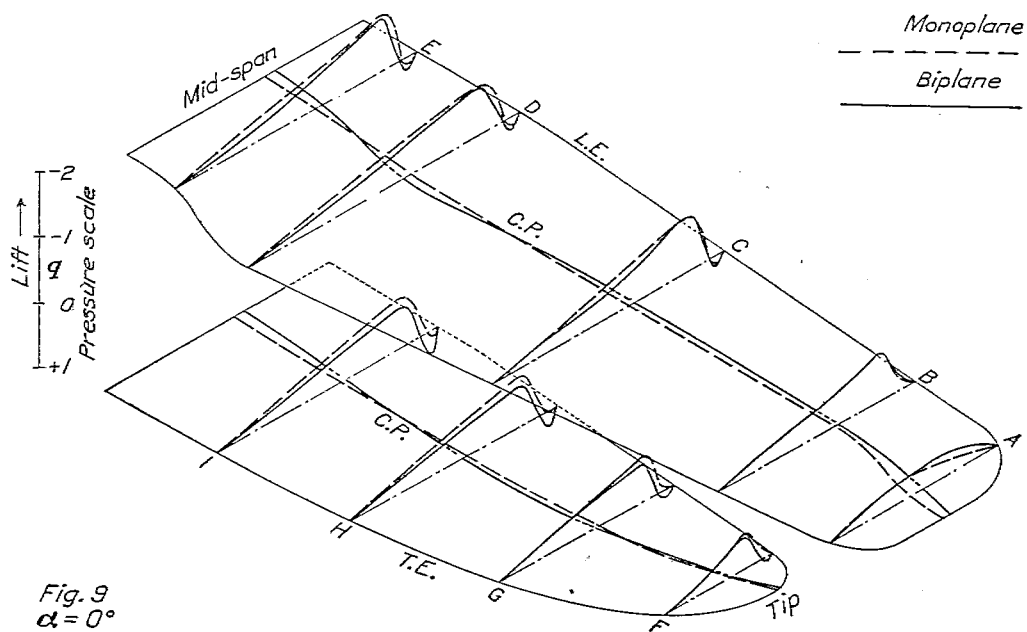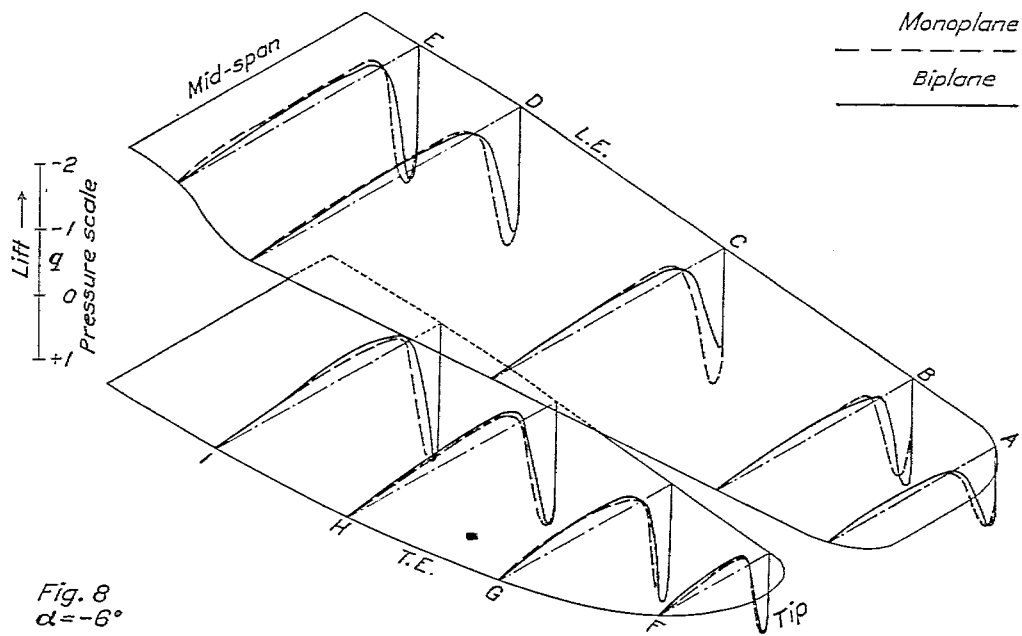
Fig. 6
$\alpha = -18°$

Fig. 7
$\alpha = -12°$

FIGS. 6 and 7.—Total normal pressure distribution

Fig. 8
$\alpha = -6°$

Fig. 9
$\alpha = 0°$

FIGS. 8 and 9.—Total normal pressure distribution
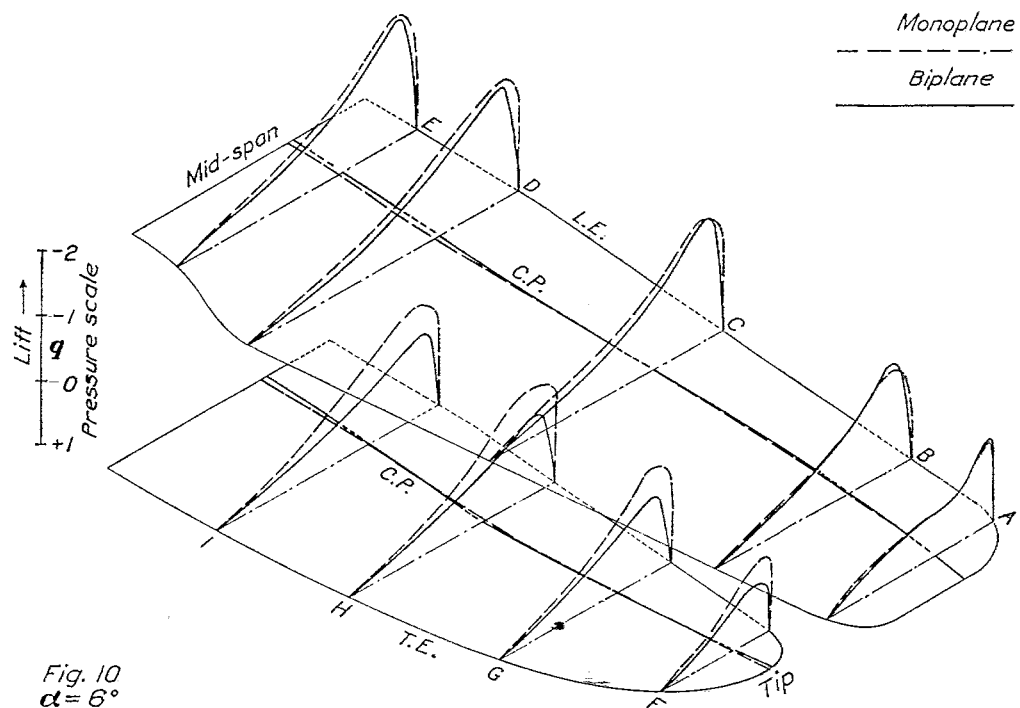
FIGS. 10 and 11.—Total normal pressure distribution

Fig. 12
α = 18°

Fig. 13
α = 21°
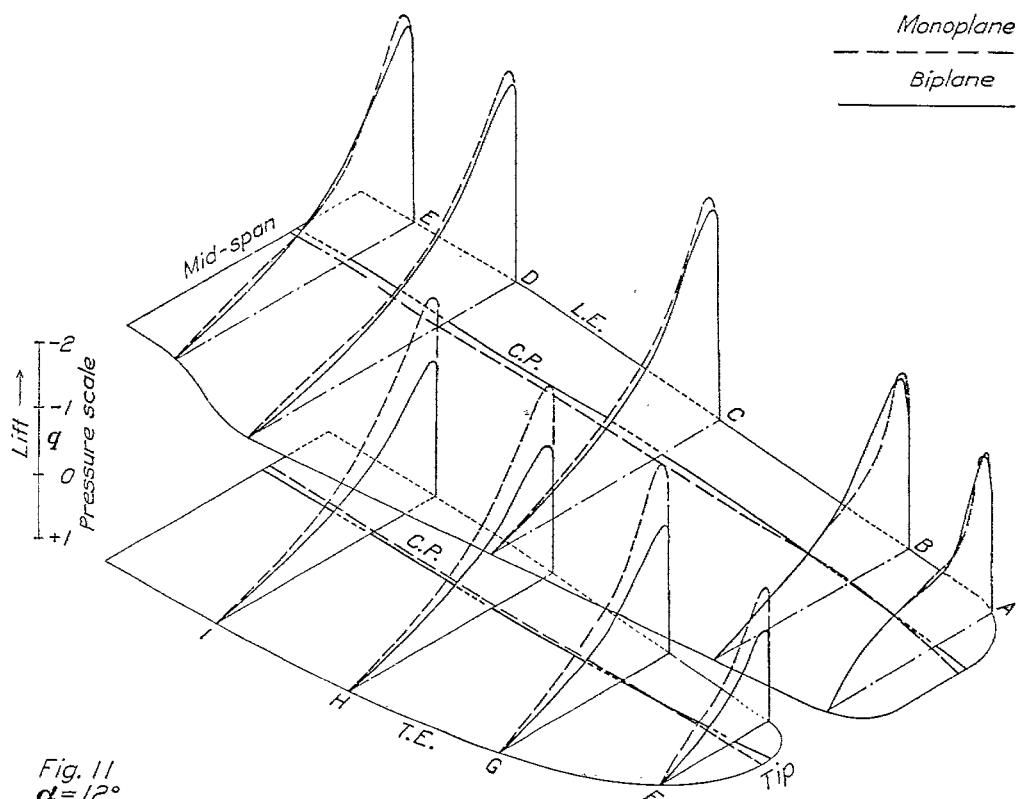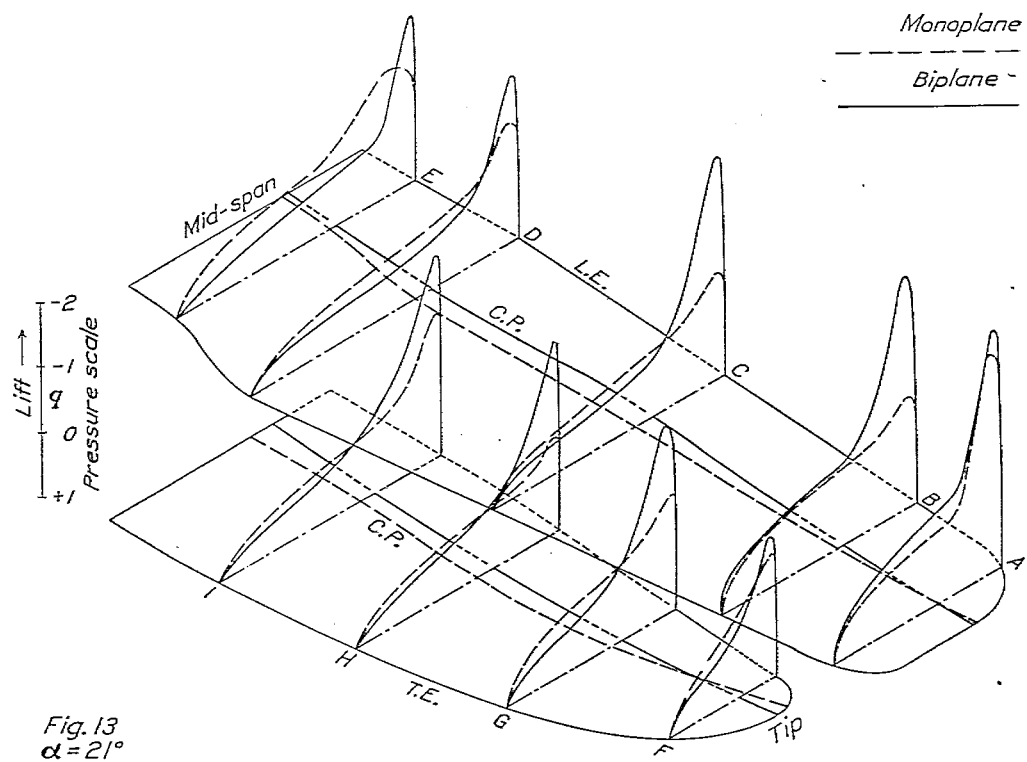
FIGS. 12 and 13.—Total normal pressure distribution

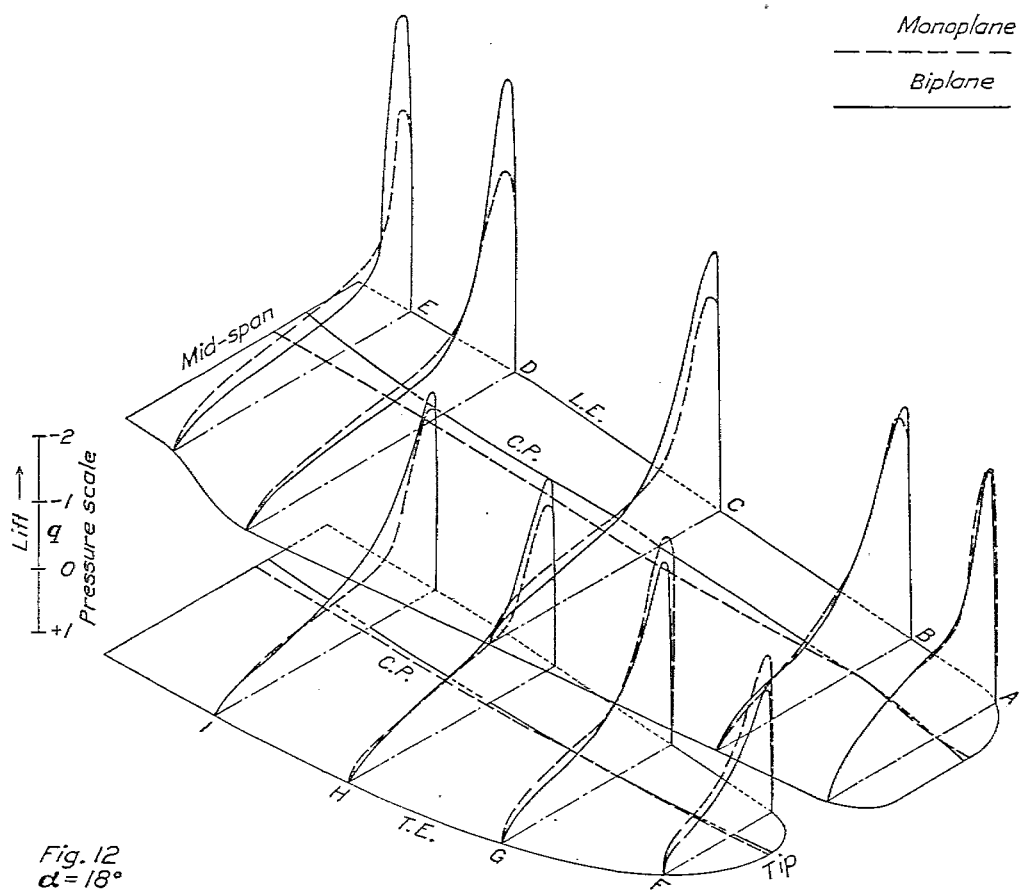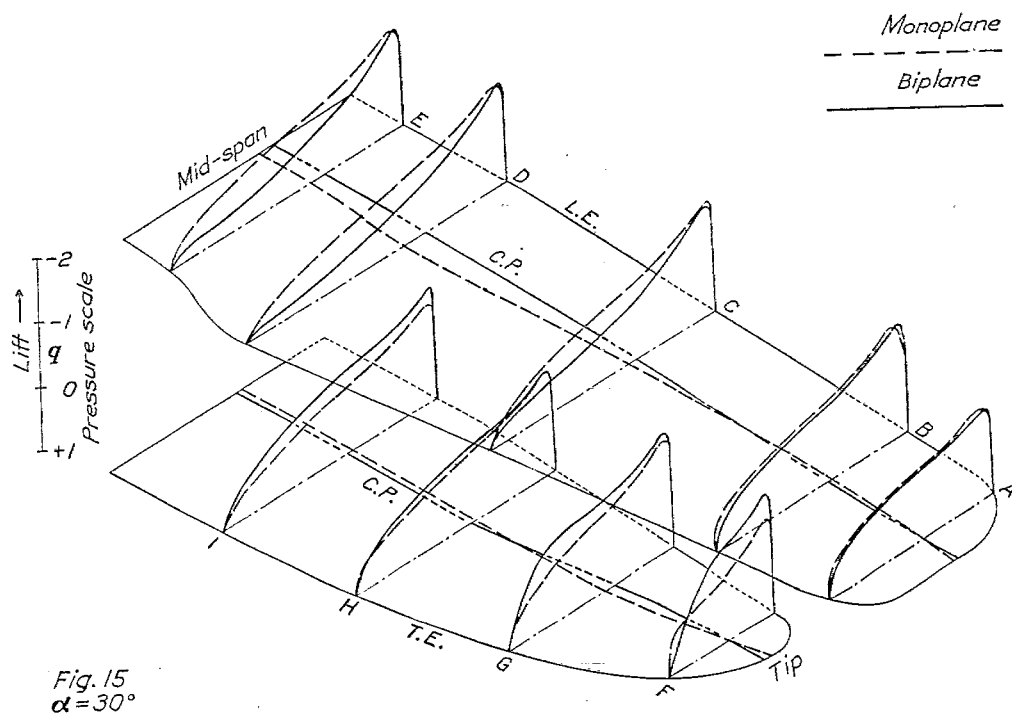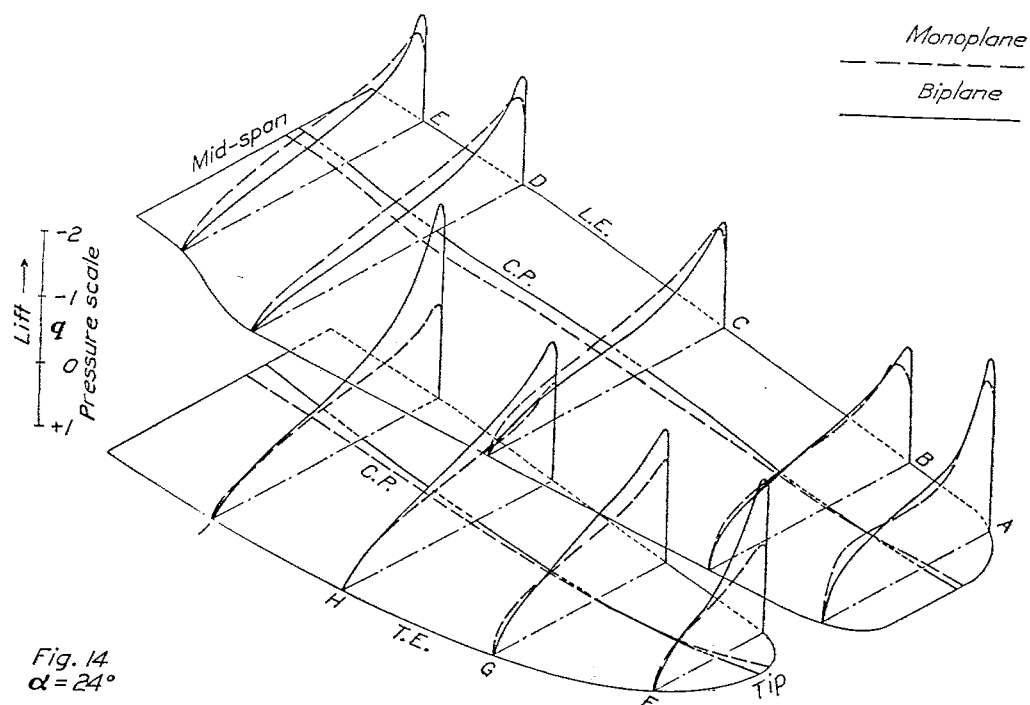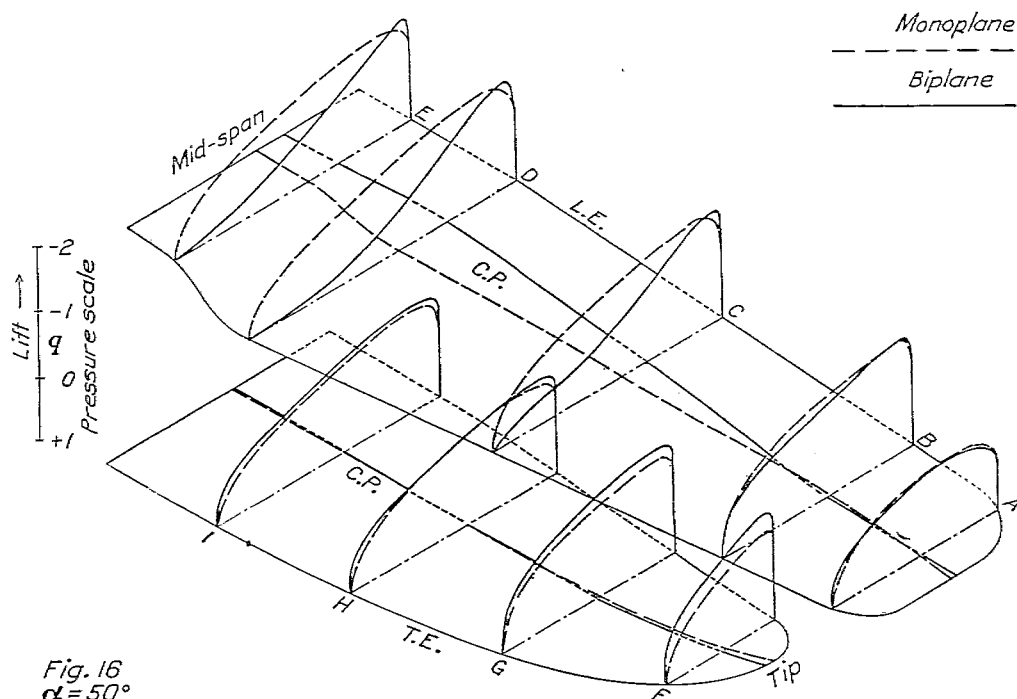Figs. 14 and 15.—Total normal pressure distribution

Fig. 16
$\alpha = 50°$
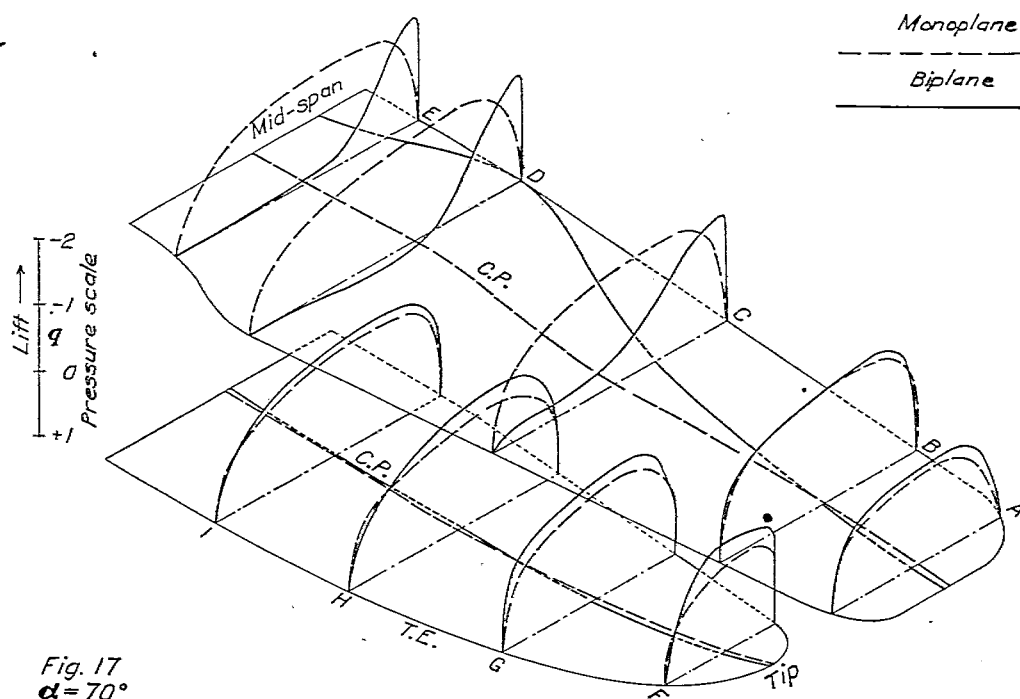

Fig. 17
$\alpha = 70°$

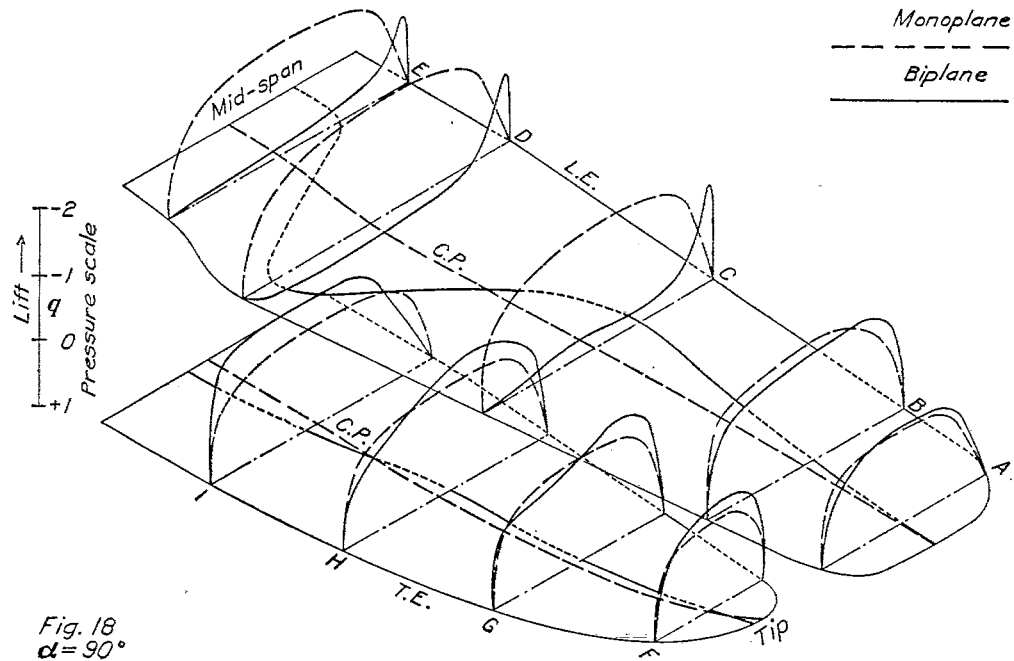FIGS. 16 and 17.—Total normal pressure distribution

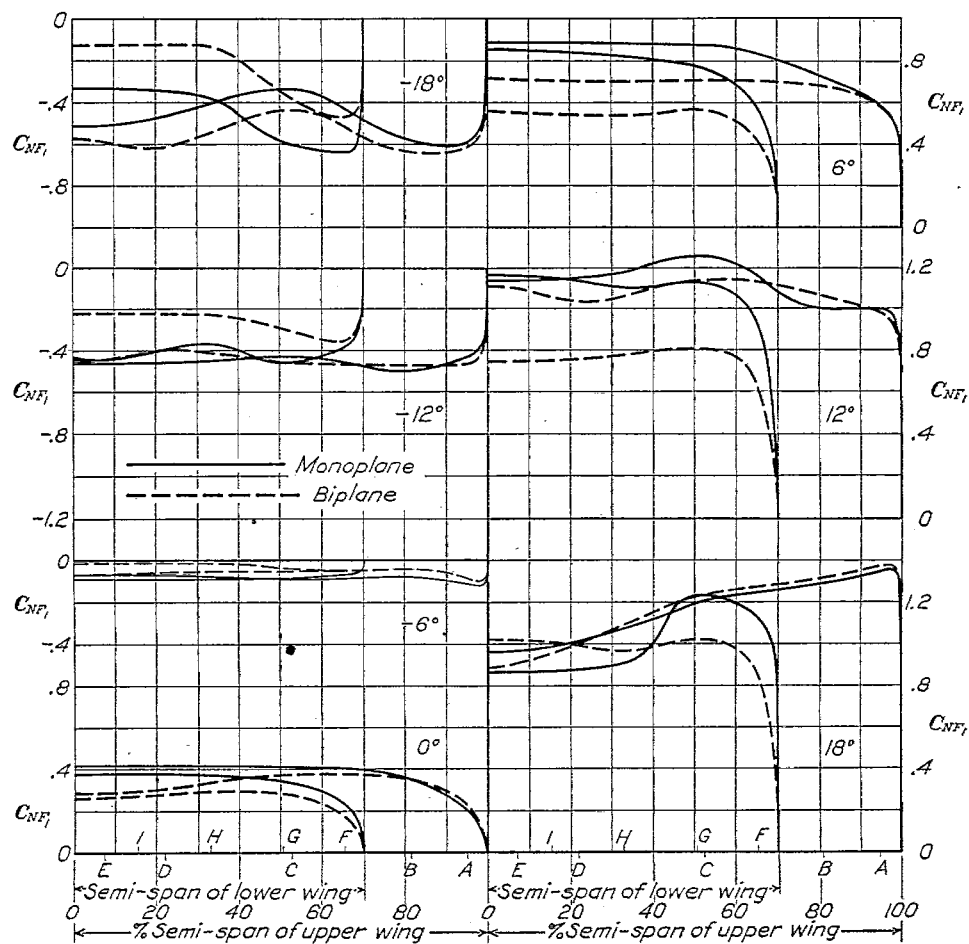FIG. 18.—Total normal pressure distribution
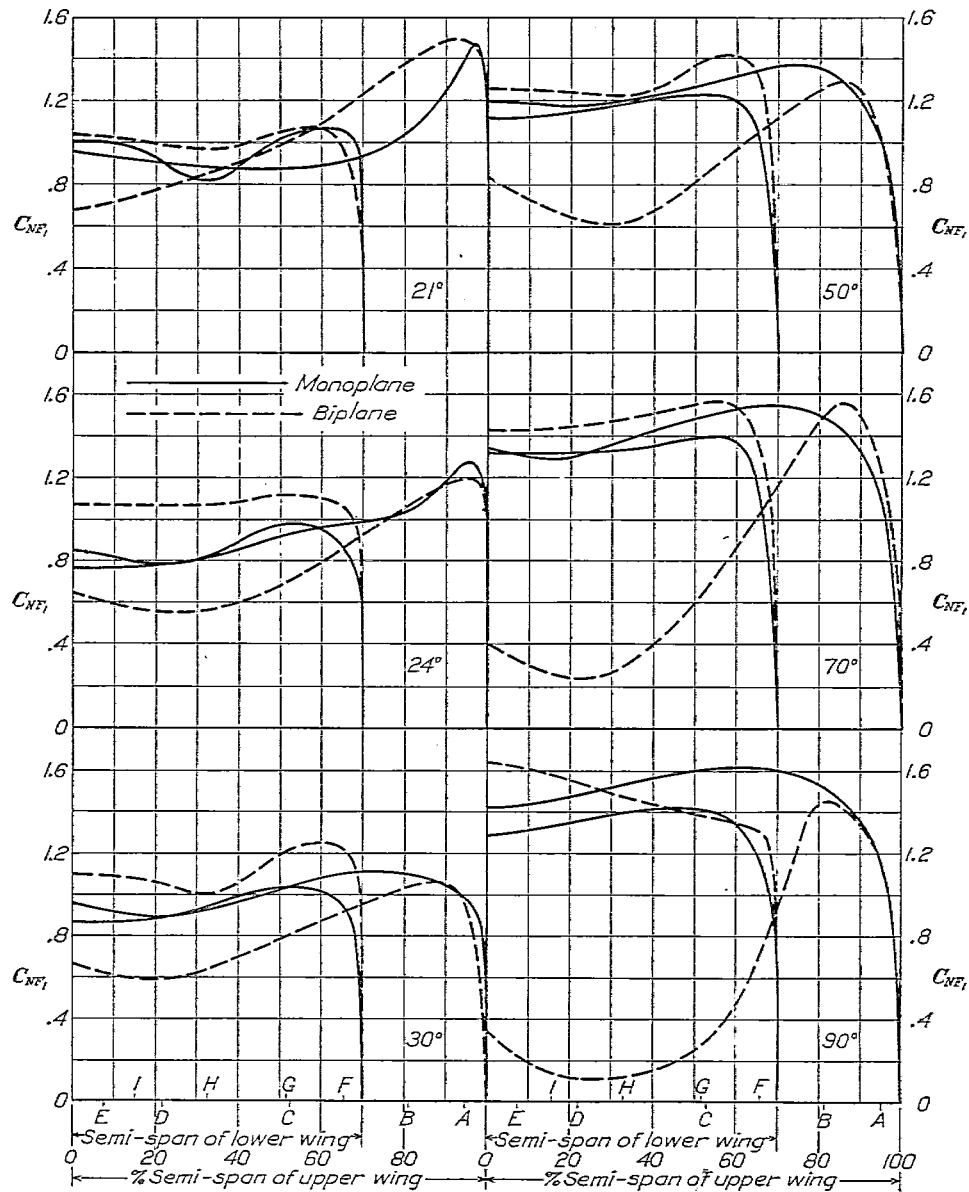

FIG. 19.—Coefficient of normal force vs. semispan

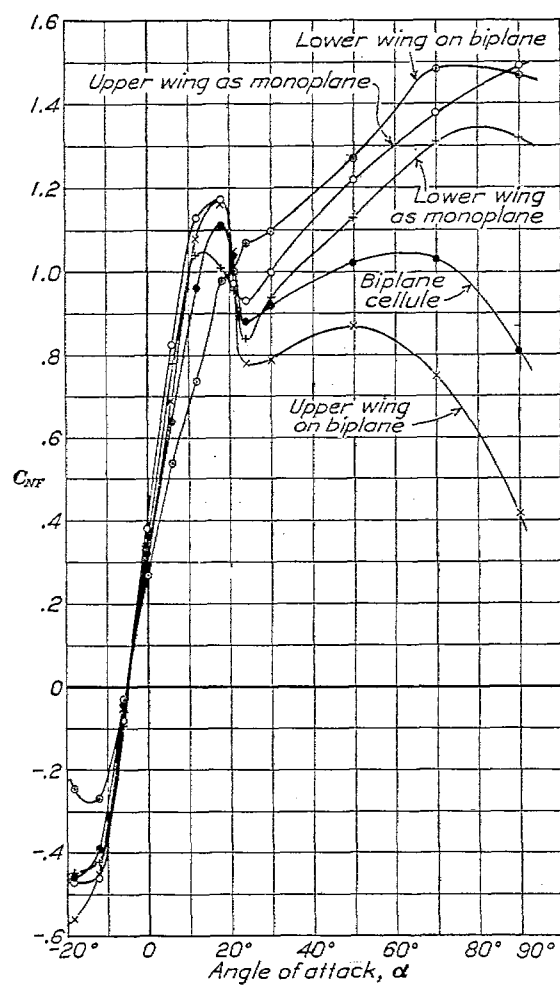FIG. 20.—Coefficient of normal force vs. semispan

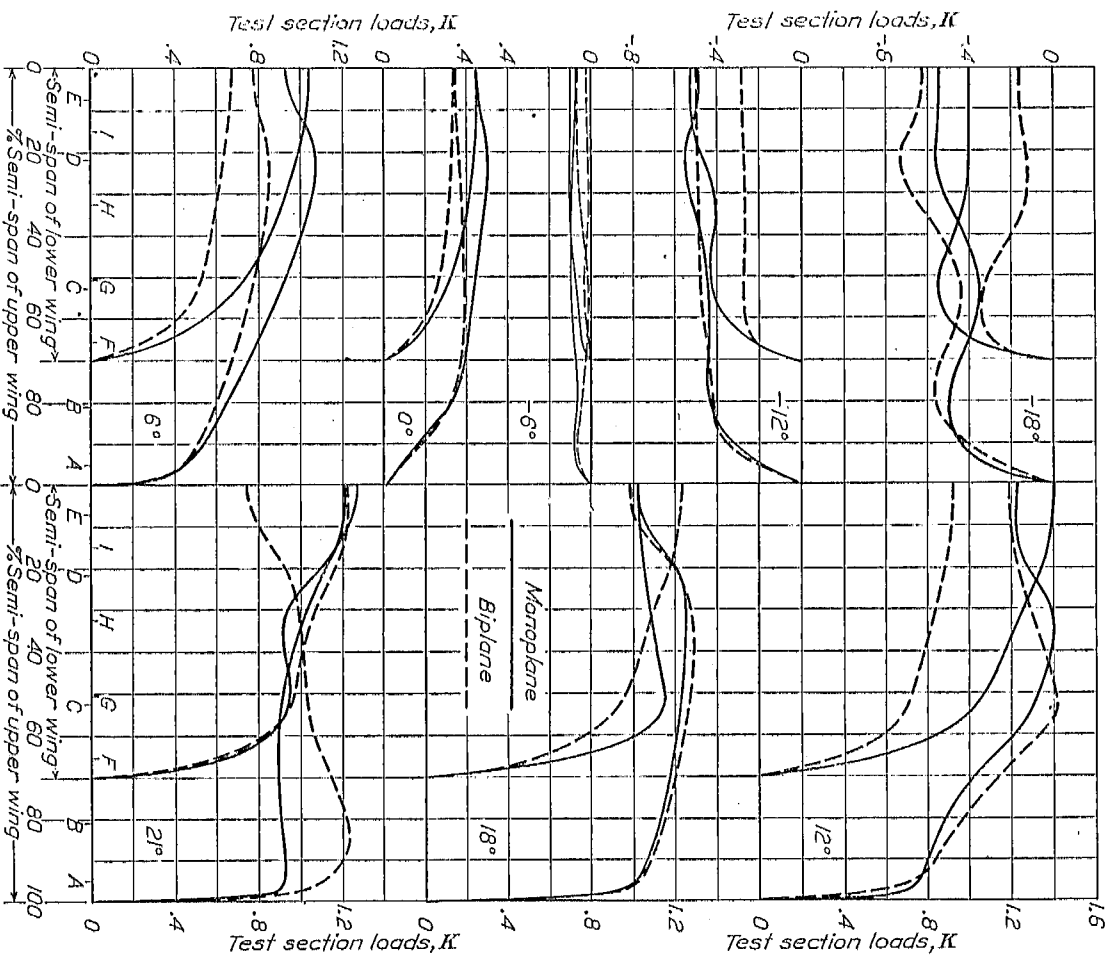FIG. 21.—Coefficient of normal force vs. angle of attack
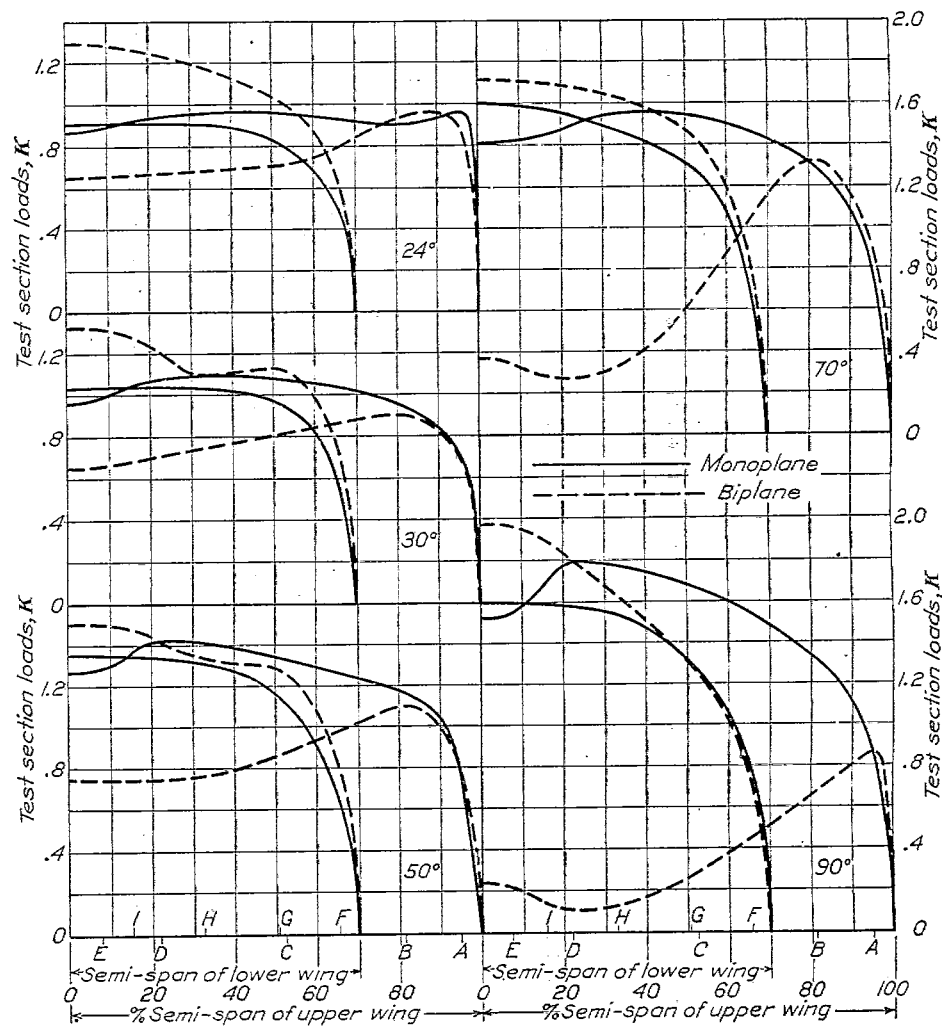
Fig 22.—Semispan loading

FIG. 23.—Semispan loading

Figure 25 illustrates the lateral C_p travel. The values for the biplane cellule were obtained from the integrated moments of the span-loading curves, by computing the equivalent moment arm of the forces on the wings measured from the plane of symmetry:

$$C_{p_b} = \frac{M_u + M_l}{A_u + A_l}$$

M_u = integrated moment of upper wing span-loading curve about the plane of symmetry.
M_L = integrated moment of the lower wing span-loading curve about the plane of symmetry.
A_u = area under K curve for upper wing.
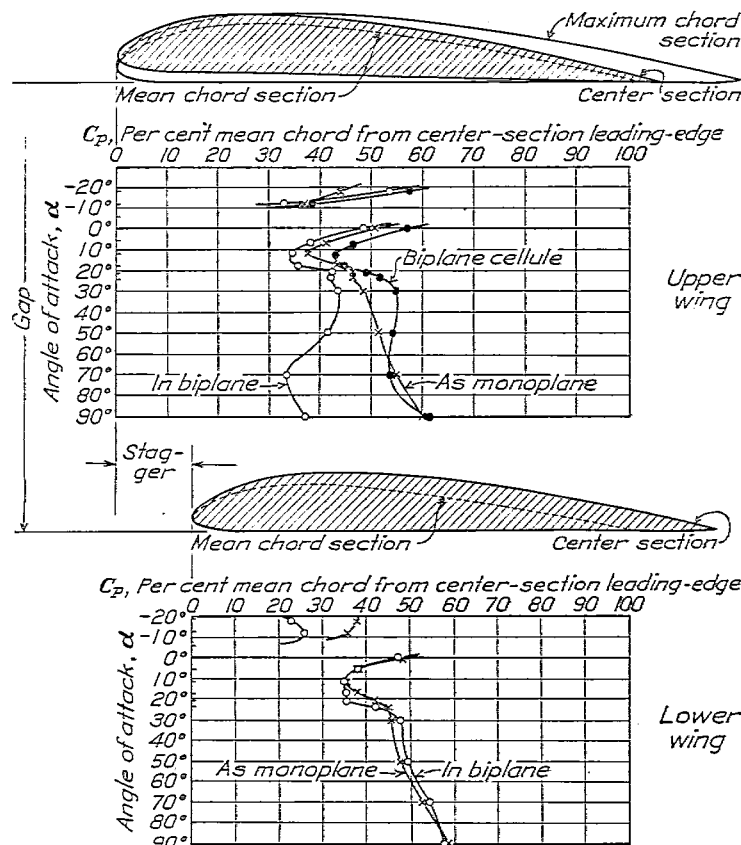A_L = area under K curve for lower wing.

FIG. 24.—Longitudinal C_p travel vs. angle of attack

DISCUSSION

At large negative angles of attack (α) the biplane upper wing pressures are greater than for the wing as a monoplane. This difference decreases as α approaches the angle of zero lift, approximately $-5°$, above which the monoplane pressures become larger than the biplane pressures. There is but slight difference in pressures between the monoplane and biplane upper wing from zero lift to maximum lift, where the biplane leading edge pressures again become larger. As α is increased beyond maximum lift, the effect of shielding of the upper wing by the lower becomes apparent and is very marked at the higher angles of attack as shown by the decided decrease in pressure on the biplane upper wing.

The influence of the upper wing on the lower at large negative angles of attack is shown by the decreased pressure on the lower wing. As α approaches zero lift the lower biplane wing and monoplane pressure diagrams become quite similar. Above zero lift the biplane pressures decrease with reference to the monoplane up to the region of maximum lift, beyond which the lower wing pressures are again higher. As seen from Figures 13, 14, and 21, these increased

pressures are due to the delayed burbling of the lower wing, a result of the influence of the upper wing. At high angles of attack the upper wing of the biplane deflects the air downward over the upper surface of the lower wing, thus tending to prevent the separation of flow from that surface.

In the region above zero lift and below maximum lift the mutual interference of the biplane wings causes decreased pressures on both wings, with the greater effect on the lower wing.

The overhanging portion of the upper wing is little affected by the lower wing of the biplane, except for an increase in pressure on the upper wing leading edge in the region of maximum lift.
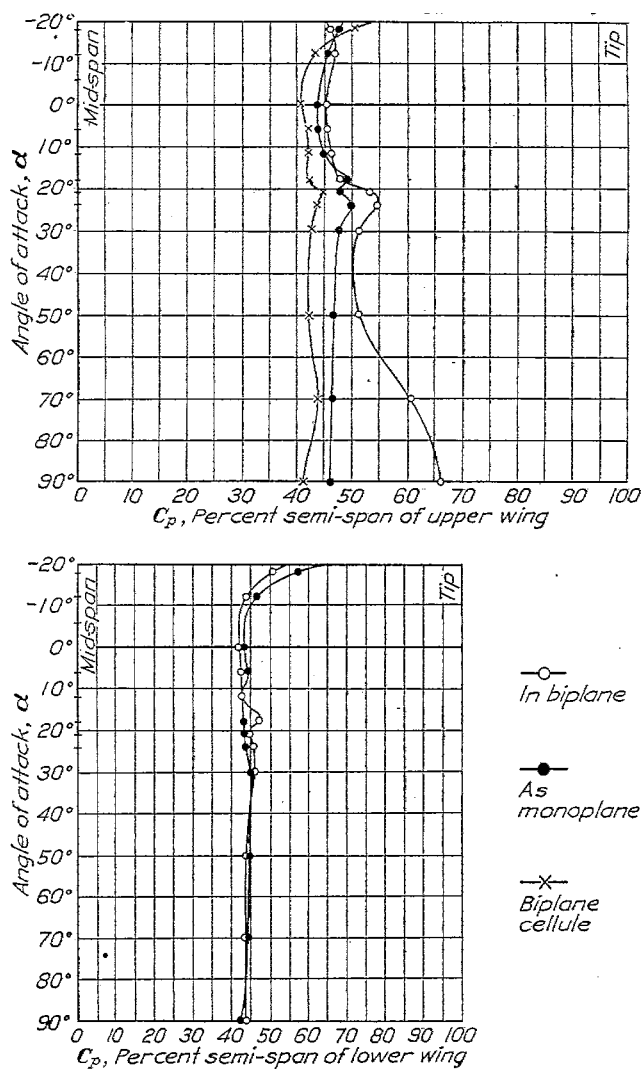

FIG. 25.—Lateral C_P travel vs. angle of attack

The longitudinal center of pressure position of the biplane upper wing is decidedly forward of that for the monoplane. That for the lower wing is but little affected, except for a slight movement to the rear at large angles of attack. (Fig. 24.)

In the biplane upper wing the lateral C_p in general moves outward with increase of angle of attack, due to the decreased pressures over the greater part of the wing, while the overhanging portion pressures are little affected by the lower wing. (Fig. 25.) The C_p of the biplane lower wing differs little from that when taken as a monoplane. Due mainly to the shorter lower wing, the biplane cellule C_p is nearer the plane of symmetry than that of the upper wing as monoplane.

CONCLUSIONS

A comparison of the biplane and monoplane results leads to the following conclusions:

1. The biplane upper wing is shielded by the lower at large angles of attack, with resulting decrease in pressures on the upper wing.

2. The influence of the biplane upper wing on the lower is marked at large negative angles of attack by decreased pressures and at large positive angles of attack by the delayed burble of the lower wing.

3. In the region above zero lift and below maximum lift the mutual interference of the biplane wings causes decreased pressures on both wings, with the greater effect on the lower wing.

4. The overhanging portion of the biplane upper wing is little affected by the lower wing, other than for slightly increased leading edge pressures in the region following maximum lift.

5. At angles of attack above maximum lift the biplane upper wing center of pressure moves forward and outward, while the C_p for the lower wing varies but little from that of the monoplane.

LANGLEY MEMORIAL AERONAUTICAL LABORATORY,
    NATIONAL ADVISORY COMMITTEE FOR AERONAUTICS,
        LANGLEY FIELD, VA., *April 9, 1928.*

BIBLIOGRAPHY

Reference 1. Reid, Elliott G.: Standardization Tests of N. A. C. A. No. 1 Wind Tunnel.   N. A. C. A. Technical
Report No. 195.
Reference 2. Fairbanks, A. J.: Pressure Distribution Tests on PW–9 Wing Models Showing Effects of Biplane
Interference.   N. A. C. A. Technical Report No. 271, 1927.
Reference 3. Warner, E. P.: Airplane Design, Aerodynamics.   Pages 41 to 49, 1927.

Fairbanks, A. J.: Distribution of Pressure Over a Model of the Upper Wing and Aileron of a Fokker
D=VII Airplane.   N. A. C. A. Technical Report No. 254, 1927.

Reid, Elliott G.: Pressure Distribution Over Thick Tapered Airfoils, N. A. C. A. 81, U. S. A. 27C Modified,
and U. S. A. 35.   N. A. C. A. Technical Report No. 229, 1926.

Norton, F. H., and Bacon, D. L.: Pressure Distribution Over Thick Airfoils—Model Tests.   N. A. C. A.
Technical Report No. 150, 1922.

Parkin, J. H., Shortt, J. E. B., and Heard, C. G.: Pressure Distribution Over U. S. A. 27 Aerofoil With
Square Wing Tips.   University of Toronto Aeronautical Research Paper No. 18, 1925.

Parkin, J. H., Shortt, J. E. B., and Code, J. G.: Pressure Distribution Over a Göttingen 387 Aerofoil with
Square Wing Tips.   University of Toronto Aeronautical Research Paper No. 18a, 1926.

Irving, H. S., and Batson, A. S.: The Distribution of Pressure Over a Biplane of Unequal Chord and Span.
British Aeronautical Research Committee Reports and Memoranda No. 997, 1925.

354